JOURNAL OF VIROLOGY, Dec. 2008, p. 12312–12324 Vol. 82, No. 24
0022-538X/08/$08.00+0 doi:10.1128/JVI.00968-08

Enhancement by Tumor Necrosis Factor Alpha of Dengue Virus-Induced Endothelial Cell Production of Reactive Nitrogen and Oxygen Species Is Key to Hemorrhage Development[▽]

Yu-Ting Yen,[1] Hseun-Chin Chen,[1] Yang-Ding Lin,[1] Chi-Chang Shieh,[2,3] and Betty A. Wu-Hsieh[1,3]*

Graduate Institute of Immunology, National Taiwan University College of Medicine, Taipei, Taiwan[1]; Departments of Microbiology and Immunology and Pediatrics, National Cheng Kung University Medical College, Tainan, Taiwan[2]; and Division of Clinical Research, National Health Research Institute, Tainan, Taiwan[3]

Received 9 May 2008/Accepted 28 August 2008

Hemorrhage is a severe manifestation of dengue disease. Virus strain and host immune response have been implicated as the risk factors for hemorrhage development. To delineate the complex interplay between the virus and the host, we established a dengue hemorrhage model in immune-competent mice. Mice inoculated intradermally with dengue virus develop hemorrhage within 3 days. In the present study, we showed by the presence of NS1 antigen and viral nuclei acid that dengue virus actively infects the endothelium at 12 h and 24 h after inoculation. Temporal studies showed that beginning at day 2, there was macrophage infiltration into the vicinity of the endothelium, increased tumor necrosis factor alpha (TNF-α) production, and endothelial cell apoptosis in the tissues. In the meantime, endothelial cells in the hemorrhage tissues expressed inducible nitric oxide synthase (iNOS) and nitrotyrosine. In vitro studies showed that primary mouse and human endothelial cells were productively infected by dengue virus. Infection by dengue virus induced endothelial cell production of reactive nitrogen and oxygen species and apoptotic cell death, which was greatly enhanced by TNF-α. N^G-Nitro-L-arginine methyl ester and *N*-acetyl cysteine reversed the effects of dengue virus and TNF-α on endothelial cells. Importantly, hemorrhage development and the severity of hemorrhage were greatly reduced in mice lacking iNOS or $p47^{phox}$ or treatment with oxidase inhibitor, pointing to the critical roles of reactive nitrogen and oxygen species in dengue hemorrhage.

Dengue virus (DENV), a member of the family *Flaviviridae*, is a mosquito-borne virus with four serotypes (DENV-1, -2, -3, and -4). The four serotypes cause DENV epidemics in Southeast Asia, Central America, and the Pacific region (24). Clinical illnesses in humans range from a flu-like disease of dengue fever to a fulminating illness of dengue hemorrhagic fever (DHF), which can progress to dengue shock syndrome (DSS) and death (32). Severe hemorrhage with low platelet counts, plasma leakage, pleural or other effusions, and increased vascular permeability are characteristics of DHF/DSS (49). Thus, it is apparent that vascular damage plays a key role in the pathophysiology of severe dengue disease.

The endothelium forms the primary barrier of the circulatory system. Vascular damage in DHF patients is evidenced by the presence of circulating endothelial cells (CECs) in the peripheral blood (7, 10). A recent report revealed the presence of apoptotic microvascular endothelial cells in the pulmonary and intestinal tissue samples from fatal cases of DSS (37), suggesting that endothelial cell apoptosis is related to vascular damage. Both host and viral factors are known to contribute to the alteration of vascular endothelial cells in dengue disease. In examining biopsy and autopsy tissue specimens from patients who died of DHF/DSS, Jessie et al. detected DENV antigens in endothelial cells in lung and liver tissues (30), suggesting that DENV might directly interact with endothelial cells in humans. Corresponding to the observation made for human dengue hemorrhage, we previously observed that there is endothelial cell damage and apoptotic endothelial cell death in hemorrhage tissues in our mouse model (9). Those studies together strongly suggest the importance of endothelial cell apoptosis in vascular damage, prompting us to examine the relationships between DENV and endothelial cells in mouse tissue as well as in vitro and to study the mechanism of endothelial cell apoptosis.

The critical role of tumor necrosis factor alpha (TNF-α) in the cause of severe dengue disease has long been recognized. Bethell et al. previously observed a positive relationship between high soluble TNF receptor levels and the severity of DHF (3a). Single-nucleotide polymorphism analysis also identified TNF-α polymorphisms at the TNF-308A allele to be a possible risk factor for hemorrhagic manifestations in patients infected with DENV (15, 39). The direct causal relationship between TNF-α and dengue hemorrhage was established in our mouse model, in that TNF-α deficiency greatly diminishes hemorrhage development (9). However, how TNF-α, together with DENV, causes endothelial cell damage remains a question to be addressed.

In this study, we investigated the molecular mechanism of dengue hemorrhage in the mouse model that we established. Our study established the temporal relationships between DENV infection of endothelial cells, the presence of TNF-α, the production of reactive nitrogen species (RNS) and reactive oxygen species (ROS), endothelial cell apoptosis, and hemorrhage development. We found that endothelial cell expression

* Corresponding author. Mailing address: Graduate Institute of Immunology, National Taiwan University College of Medicine, No. 1 Jen-Ai Road, Section 1, Taipei, Taiwan. Phone: 886-2-2321-7510. Fax: 886-2-2321-7921. E-mail: bwh@ntu.edu.tw.

▽ Published ahead of print on 8 October 2008.

of inducible nitric oxide synthase (iNOS) and tyrosine nitration are characteristic of hemorrhage tissues. Moreover, deficiencies in iNOS or $p47^{phox}$, a cytosolic component of NADPH oxidase (26), and an oxidase inhibitor reduces hemorrhage development in DENV-infected mice. The results of this study point to the roles of RNS and ROS in the pathogenesis of dengue hemorrhage.

MATERIALS AND METHODS

Mice and DENV infection. DENV-2 strain 16681 was used throughout this study (9). C57BL/6 $iNOS^{-/-}$ ($Nos2^{tm1Lau}$/J) mice were originally obtained from the Jackson Laboratory (Bar Harbor, ME) and bred at the Laboratory Animal Center of the National Taiwan University College of Medicine. Male $p47^{phox-/-}$ [B6(Cg)-Ncf^{1m1J}/J] mice were obtained from the Jackson Laboratory and housed in microisolator cages in pathogen-free and environmentally controlled conditions at the Laboratory Animal Center of National Cheng Kung University. Mice were inoculated with DENV-2 strain 16681 (in 0.4 ml) intradermally at four sites (as four corners of a rectangle) on the upper back as described previously (9). Mice given phosphate-buffered saline (PBS) or UV-inactivated DENV through the same route were used as controls. At 3 days after infection, mice were killed, and all tissues were examined to observe hemorrhage development.

In vivo treatment with inhibitors. To inhibit the effect of ROS, animals were fed with drinking water containing 40 μg/ml apocynin (Sigma-Aldrich, St. Louis, MO) 5 days before DENV inoculation and continued until the termination of the experiment. Apocynin was dissolved in absolute ethanol and diluted to1:2,000 in sterilized water (25). The final concentration of ethanol (vehicle) in the drinking water was 0.05%. The drinking water containing apocynin was replenished daily and protected from light. The irreversible pancaspase inhibitor BOC-Asp(OMe)-fluoromethyl ketone (Boc-D-FMK) (Sigma-Aldrich) and the control peptide Z-Phe-Ala-fluoromethyl ketone (Z-FA-FMK) (Sigma-Aldrich) were dissolved in dimethyl sulfoxide (DMSO) and administered to mice through intraperitoneal injection at 10 μmol/kg (1). The final concentration of DMSO was 0.05%. Mice were treated daily, beginning at the day of infection, until the termination of the experiment.

Staining for DENV NS1 antigen. To detect viral NS1 expression, subcutaneous tissues were collected from mice at 6, 12, and 24 h after intradermal inoculation with 4×10^7 PFU of DENV. Cryosections were fixed in 4% paraformaldehyde for 10 min at room temperature before a 1-h treatment with mouse-on-mouse (MOM) mouse immunoglobulin G (IgG) blocking reagent (Vector, Burlingame, CA). Sections were then stained with mouse anti-DENV NS1 antibody (a gift from Huan-Yao Lei, National Cheng Kung University, Tainan, Taiwan) in MOM diluent and fluorescein isothiocyanate (FITC)-conjugated rat anti-mouse CD31 antibody at 4°C overnight. Alexa Fluor 594-conjugated goat anti-mouse IgG antibody (Jackson Immunoresearch, West Grove, PA) in MOM diluent was added. Naïve mouse serum plus Alexa Fluor 594-conjugated goat anti-mouse Ig and FITC-conjugated rat anti-mouse IgG2a were used as controls. Hoechst 33258 stain (Sigma-Aldrich) was used to stain nuclei.

In situ hybridization. The in situ hybridization method was adopted from methods reported previously (23, 40). In brief, tissue cryosections were first washed in absolute ethanol and dried at room temperature before treatment with proteinase K (100 μg/ml) at 37°C for 15 min. The probe 5′-CTG-ATT-TCC-AT(ACGT)-CC(AG)-TAX-biotin-3′ at 2 ng/μl was pipetted onto the tissue sections or monolayer before incubation at 45°C for 20 h. Probes that had hybridized with viral RNA were detected by use of horseradish peroxidase (HRP)-conjugated anti-biotin antibody. Diaminobenzidine (DAB) was used as a substrate for color development.

Detection of TNF-α and iNOS mRNA in tissues by reverse transcription (RT)-PCR. Total RNA was extracted from skin tissues using Trizol reagent (Invitrogen, Carlsbad, CA) according to the method described previously (9). The amplification condition was 90°C for 3 min, followed by 35 cycles of 94°C for 40 s, 69°C for 1 min, 72°C for 1 min, and then 72°C for 10 min, and the reaction was stopped at 4°C. The PCR products were subjected to electrophoresis on a 2% agarose gel. The sequences of the iNOS primer set were 5′-TGGGAATGGAGA CTGTCCCAG-3′ and 5′-GGGATCTGAATGTGATGTTTG-3′ (44), and those for TNF-α primers were 5′-ATCCGCGACCTCGCCCTG-3′ and 5′-ACCGCCTG GAGTTCTGGAA-3′. The sequence for the hypoxanthine phosphoribosyltransferase (HPRT) primer set was 5′-GTTGGATACAGGCCAGACTTTGTTG-3′ and 5′-GAGGGTAGGCTGGCCTATGGCT-3′ (9).

Hematoxylin and eosin staining. Tissues were fixed in 4% neutral formalin solution, embedded in paraffin, and sectioned at a 3-μm thickness. After deparaffinization and rehydration, the sections were stained with hematoxylin and eosin. The sections were dehydrated before mounting.

Flow cytometric analysis of CECs. Peripheral blood was collected from mice, and the red blood cells were lysed in BD FACS lysing solution (BD Bioscience, San Jose, CA) and stained with FITC-conjugated rat anti-mouse CD31 (clone PECAM-1), allophycocyanin-conjugated rat anti-mouse vascular endothelial cell growth factor 2 (VEGFR2) (clone 89B3A5), and PE/Cy7-conjugated rat anti-mouse CD45 (clone 30-F11) (all from BioLegend, San Diego, CA) antibodies. Cells were acquired by use of a FACSCanto flow cytometer (BD Biosciences) and analyzed by BDFACSDiva flow cytometric analysis software (BD Biosciences). Platelets and cellular debris were excluded.

In situ detection of DNA fragmentation. DNA strand breaks were end labeled with dUTP by terminal deoxynucleotidyl transferase (TdT) using an In Situ Cell Death Detection kit (Roche Applied Science, Indianapolis, IN) (9). To detect endothelial cell apoptosis in tissues, cryosections were fixed in 4% paraformaldehyde at room temperature for 10 min and then treated with 3% H_2O_2 in methanol. Cryosections were then washed and treated with 0.1% Triton X-100 in 0.1% sodium citrate on ice for 2 min. The TdT-mediated dUTP nick end labeling (TUNEL) reaction mixture of enzyme solution (TdT) and label solution (fluorescein-labeled nucleotides) was added and placed at 37°C for 1.5 h. Phycoerythrin (PE)-conjugated rat anti-mouse CD31 antibody was added and left at 4°C for 1 h. Hoechst 33258 stain was added after washing. To detect cell death in the primary endothelial cell monolayer, converter-POD (peroxidase-conjugated anti-fluorescein antibody) was added, and DAB was used as a substrate for color development.

Immunofluorescence staining. Tissues were snap-frozen in liquid nitrogen, and the cryosections were fixed in acetone for 5 min and then blocked by treatment with PBS containing 5% goat serum at room temperature for 20 min. To observe the relationship between macrophages and endothelial cells, sections were stained with both PE-conjugated rat anti-mouse CD31 and FITC-conjugated rat anti-mouse F4/80 (clone BM8; eBioscience) antibodies at 4°C overnight. To detect iNOS expression in endothelial cells, sections were stained with both polyclonal FITC-conjugated rabbit anti-mouse iNOS (BD Pharmingen) and PE-conjugated rat anti-mouse CD31 antibodies at 4°C overnight. To detect endothelial cell expression of nitrotyrosine, sections were stained with primary rabbit anti-nitrotyrosine (Upstate Biotechnology, Inc., Lake Placid, NY) and PE-conjugated rat anti-mouse CD31 antibodies simultaneously at 4°C, and secondary FITC-conjugated goat anti-rabbit Ig antibody was added after overnight incubation. To detect endothelial cell expression of DENV antigen, skin, subcutaneous, and intestinal tissues were stained with polyclonal rabbit anti-DENV antibody (kindly provided by Wen Chang, Institute of Molecular Biology, Academia Sinica, Taipei, Taiwan) and PE-conjugated anti-rabbit Ig (Invitrogen) as described previously (9). Hoechst 33258 stain was used as a counterstain.

Infection of endothelial cells with DENV. Human umbilical vein endothelial cells (HUVECs) were prepared as previously described (27). The method of isolating mouse brain microvascular endothelial cells (MBECs) was adopted from a previously published protocol (53). HUVECs and MBECs at passages 3 to 5 and 2 to 4, respectively, were used in experiments. About 5×10^4 endothelial cells (HUVECs or MBECs) were seeded onto 13-mm round coverslips (Polylab, Strasbourg, France) precoated with 1% gelatin. After overnight incubation, the cells were cultured in medium containing 2% inactivated fetal bovine serum before different titers of live or UV-inactivated DENV were added. The cells were incubated at 37°C for 2 h with gentle shaking every 10 min. After washing, the cells were cultured in medium containing 10% inactivated serum, the culture supernatants were harvested for NOx (mixture of NO^-, NO_2^-, and NO_3^-) determination and plaque assay (9), and infected endothelial cells were harvested for viral antigen determination.

In vitro treatment with inhibitors. The caspase inhibitor benzyl-oxycarbonyl-valyl-alanylaspartic acid fluoro-methyl ketone (zVAD-FMK) (4 μM; Clontech Laboratories, Palo Alto, CA), ceramide inhibitor fumonisin B_1 (Cayman, Ann Arbor, MI), or RNS inhibitor *N*-nitro-L-arginine methyl ester (L-NAME) (10 nM; Clontech Laboratories), singly or in combination with ROS inhibitor *N*-acetyl cysteine (NAC) (15 nM; Sigma-Aldrich), was added to endothelial cell cultures 30 min before DENV was added and left in the culture throughout the experiment.

Cell viability determination. The viability of HUVECs after DENV infection was quantified by their ability to reduce 3-[4,5-dimethylthiazol]-2,5-diphenyltetrazolium bromide (MTT) to formazan precipitate in quadruplicate wells. MTT (Sigma-Aldrich) at a final concentration of 5 mg/ml was added to each well 3 h before the termination of the experiment. Formazan dye was dissolved by incubation in DMSO (Merck, Berlin, Germany), and its concentration was determined spectrophotometrically at an absorbance wavelength of 560 nm. The percentage of cell death was calculated based on the optical density at 560 nm

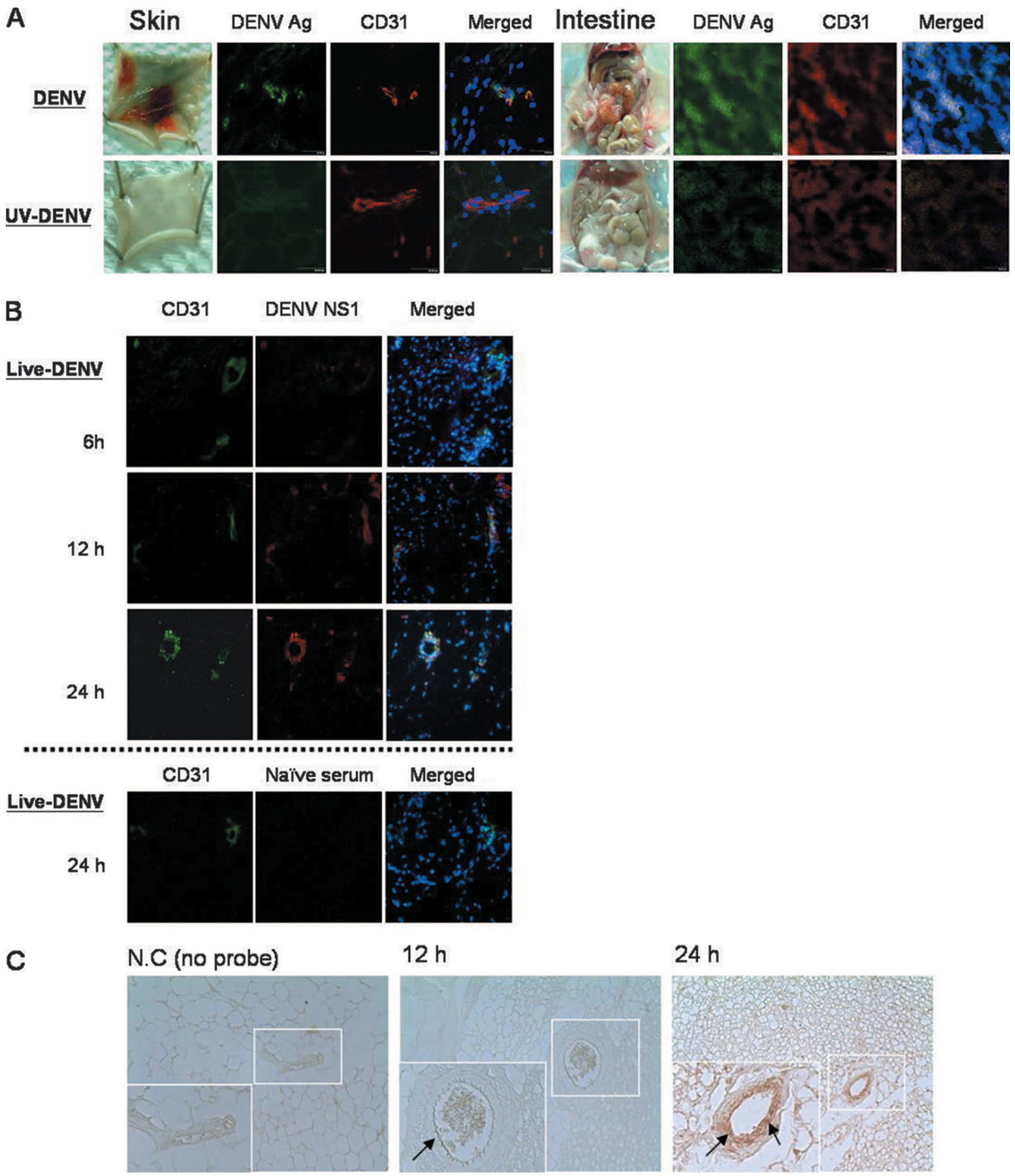

FIG. 1. DENV antigen (Ag) and nucleic acids are detectable in endothelial cells of hemorrhage tissues after intradermal infection. (A) Mice were inoculated intradermally with 2×10^9 PFU of viable DENV or an otherwise equivalent titer of UV-inactivated DENV at four different sites in the back. The skin and the intestine were exposed and harvested at 3 days after infection. The cryosections of the hemorrhagic skin and intestine were stained with rabbit anti-DENV antiserum plus FITC-conjugated goat anti-rabbit IgG, PE-conjugated rat anti-mouse CD31 antibody, and Hoechst 33258 stain. Original magnification, ×630. The data shown are representative of four repeated experiments. (B) The cryosections of subcutaneous tissues collected from mice intradermally infected with viable DENV (4×10^7 PFU) at 6, 12, and 24 h after inoculation were stained with mouse anti-NS1 antibody plus Alexa Fluor 594-conjugated goat anti-mouse antibody, FITC-conjugated rat anti-mouse CD31 antibody, and Hoechst 33258 stain. Naïve mouse serum plus Alexa Fluor 594-conjugated goat anti-mouse antibody and FITC-conjugated rat anti-mouse IgG2a (isotype control) were used as staining controls. Original magnification, ×630. (C) Skin was harvested from mice intradermally infected with 4×10^7 PFU DENV at 12 and 24 h after infection. In situ hybridization was performed with a biotin-labeled DNA probe, and DENV RNA was detected by HRP-conjugated anti-biotin antibody. DAB was used as a substrate for color development. The no-probe control (N.C) was a skin section harvested 24 h after infection and stained with the biotin detection system without the probe. Arrows point to viral nucleic acid-positive endothelial cells. Original magnification, ×400.

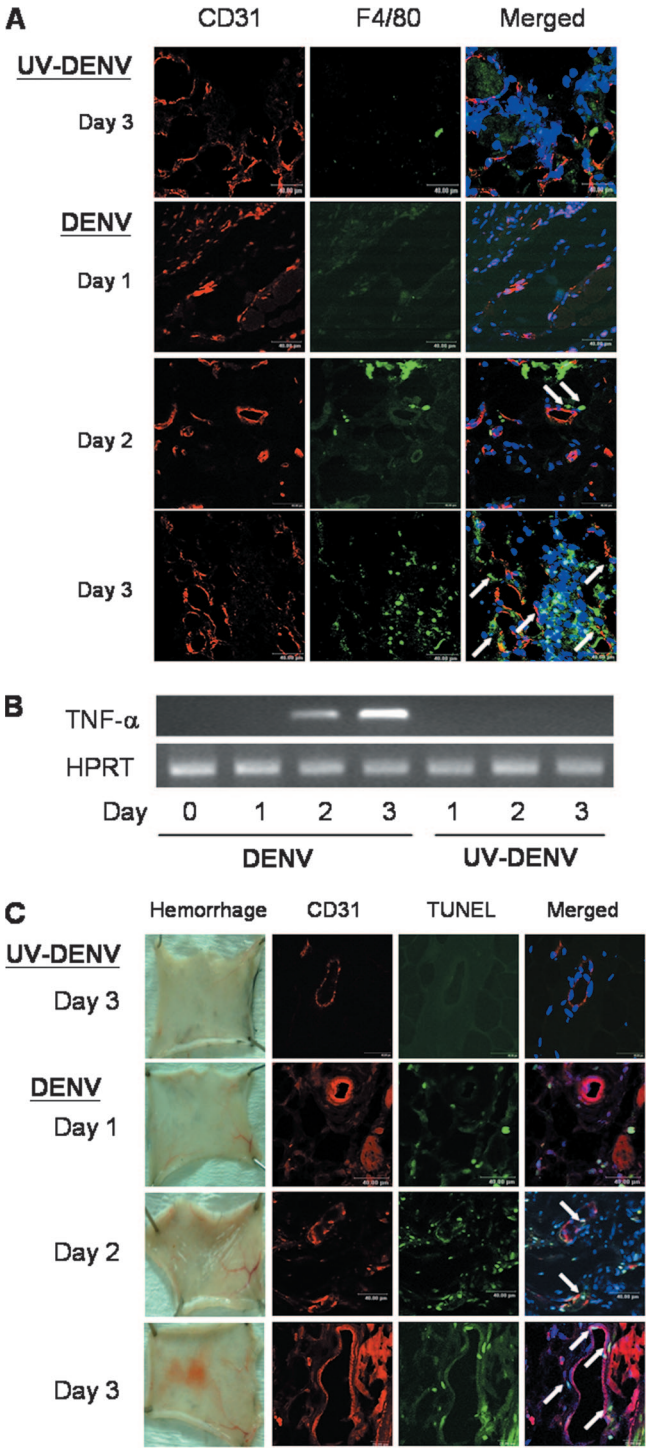

FIG. 2. Hemorrhage is accompanied by infiltrating macrophages in the vicinity of endothelial cells, TNF-α production, and endothelial cell death. Skins were harvested from mice infected with 2×10^9 PFU viable DENV or an otherwise equivalent titer of UV-inactivated DENV at days 1, 2, and 3 after infection. (A) The cryosections of the skin samples were stained with PE-conjugated rat anti-mouse CD31 and FITC-conjugated rat anti-mouse F4/80 antibodies and Hoechst 33258 stain. White arrows point to F4/80-positive macrophages in close proximity to endothelial cells. Staining with various isotype control antibodies was negative. Original magnification, ×630. Data presented are representative of three repeated experiments. (B) TNF-α mRNA was amplified by RT-PCR. The housekeeping HPRT gene was used as a control. (C) Skin samples from infected mice were exposed at days 1, 2, and 3 after infection. The cryosections of the skin samples were stained with PE-conjugated rat anti-mouse CD31 antibody, FITC-conjugated TUNEL mixture, and Hoechst 33258 stain. White arrows point to TUNEL-positive ($TUNEL^+$) $CD31^+$ cells. Original magnification, ×630. The data shown are representative of four repeated experiments.

(OD_{560}) reading by use of the following formula: Percentage of cell death = 100 × (OD_{560} of treated sample/OD_{560} of untreated sample). Assays were performed in triplicate. The standard deviation was calculated from data of obtained from separate experiments.

Determination of NOx concentrations. HUVEC culture supernatants were collected at different time intervals after infection with DENV. The Griess reagent kit for nitrite determination (Molecular Probes, Eugene, OR) was used according to the manufacturer's instructions.

Determination of free radicals. 2′,7′-Dichlorodihydrofluorescein (DCFH) diacetate (DCFH-DA; Molecular Probes) was used to determine endothelial cell production of free radicals. At 45 min after the addition of DCFH-DA (5 μM), cells were washed and resuspended in PBS. Cells were acquired by use of a FACScan flow cytometer and analyzed by use of CellQuest software (BD Biosciences) for DCF-positive cells.

Western blot analysis. Western blotting was performed as described previously (55). The primary antibodies rabbit anti-human endothelial nitric oxide synthase (eNOS) (1:1,000 dilution; Chemicon, Temecula, CA), rabbit anti-human iNOS, (1:1,000 dilution; R&D, Minneapolis, MN), and mouse anti-human α-tubulin (1:1,000 dilution; Abcam, Cambridge, MA) were used. After washing, blots were incubated with a 1/5,000 dilution of HRP-conjugated goat anti-mouse or goat anti-rabbit IgG at 4°C for 1 h. The blots were visualized using the ECL detection system (Amersham Biosciences, Buckinghamshire, United Kingdom) in accordance with the supplier's instructions.

Transendothelial permeability assay. The method of transwell experiments was adopted from a method reported in a previous publication by Bonner and O'Sullivan (6). HUVECs were grown to confluent monolayers in the upper chamber of the polycarbonate membrane transwell by seeding at 2×10^6 cells/cm^2 and incubated for 72 h. Trypan blue-labeled bovine serum albumin was prepared by adding 180 mg trypan blue (sigma) and 4 g bovine serum albumin fraction V (sigma) to 100 ml Hanks balanced solution (Gibco) and precipitated with 5% trichloroacetic acid. Cultures with or without zVAD-FMK (4 μM) treatment were infected with DENV (multiplicity of infection [MOI] of 0.1), were treated with TNF-α (300 pg/ml), received both DENV and TNF-α, or received neither. After incubation for 24 h, 100 μl of trypan blue-stained bovine serum albumin was added to the upper chamber of the transwell 30 min before the upper chambers were removed. The absorbance of the solution in the lower chamber was measured at 595 nm.

Statistical analysis. A Student's *t* test was used to compare the difference between groups. Results are reported as means ± standard deviations.

RESULTS

Dengue hemorrhage is accompanied by DENV infecting endothelial cells, macrophage infiltration, TNF-α production, and endothelial cell death. We reported in a previous publication that immunocompetent C57BL/6 mice injected intradermally with DENV-2 16681 develop hemorrhage (9). Systemic and severe hemorrhage was observed at different anatomical sites after the injection of 3×10^9 PFU of the virus (Fig. 1A) (9). Immunofluorescence staining showed that $CD31^+$ endothelial cells in the vascular endothelial cells of both the hemorrhagic skin and intestine tissues expressed DENV antigen (Fig. 1A). Results shown in Fig. 1B and C show that viral NS1 and nucleic acids can be detected at as early as 12 h in endothelial cells and continued to increase until 24 h after infection, showing that DENV actively infects and replicates in endothelial cells at an early phase of the infection (43). Interestingly, after DENV infected endothelial cells, macro-

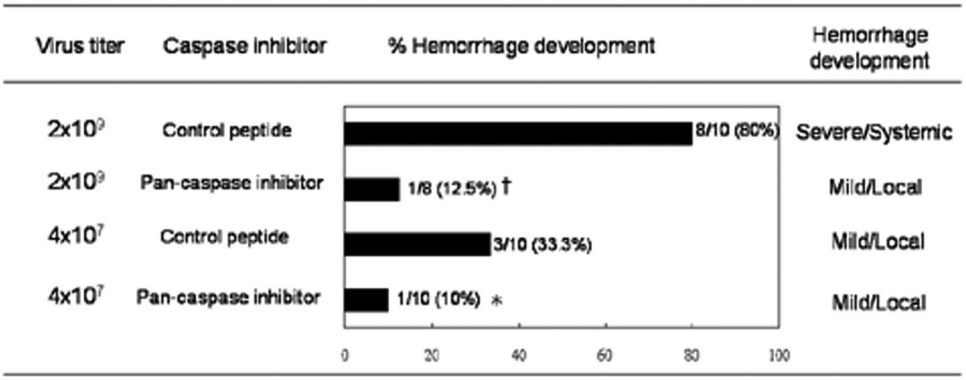

FIG. 3. Administration of caspase inhibitor reduces hemorrhage development in DENV-infected mice. Mice were inoculated intradermally with the indicated titers of viable DENV. Mice were treated with the caspase inhibitor Boc-D-FMK at 10 μmol/kg or an equivalent concentration of the control peptide Z-FA-FMK daily beginning at the day of DENV infection. Hemorrhage was observed at day 3 after DENV inoculation. †, $P < 0.001$; *, $P < 0.05$ (comparing mice treated with pancaspase inhibitor to those treated with control peptide infected with the same titer of DENV).

phages were observed in the tissues. They appeared as early as day 2 and came into the close proximity of the endothelium by day 3 of infection (Fig. 2A). Coincident with the increase in numbers of infiltrating macrophages, the level of TNF-α transcripts also increased (Fig. 2B) (9). A TUNEL reaction further revealed that endothelial cells in the hemorrhage tissues became apoptotic at days 2 and 3 after infection, before and when hemorrhage was observed (Fig. 2C). These kinetics studies demonstrate that hemorrhage development is accompanied by DENV infection of endothelial cells, macrophage infiltration, TNF-α production, and endothelial cells undergoing apoptosis (9). Furthermore, the percentage of mice that developed hemorrhage and the severity of hemorrhage were greatly reduced when mice were treated with the pancaspase inhibitor Boc-D-FMK (Fig. 3), showing the importance of apoptosis, most probably that of endothelial cells, to hemorrhage development.

By excluding $CD45^+$ leukocytes and gating $VEGFR^+$ $CD31^+$ cells in the peripheral blood, we found that in mice which developed hemorrhage, there was significantly greater numbers of CECs (Fig. 4). These data provide ex vivo evidence to show that vascular damage occurs in the hemorrhagic mice and that it can be detected by increased numbers of CECs in the circulation (14, 19, 22).

iNOS upregulation and free radical production in the endothelial cells of hemorrhage tissue. To investigate whether iNOS expression and oxygen radicals are involved in endothelial cell damage and hemorrhage development, hemorrhage tissues from DENV-infected mice were compared to tissues from mice injected with UV-inactivated DENV. RT-PCR results showed that iNOS mRNA transcripts were upregulated in the tissues of hemorrhagic mice but not in mice injected with UV-inactivated DENV (Fig. 5A). Furthermore, $CD31^+$ vascular endothelial cells in hemorrhage tissues expressed both iNOS and nitrotyrosine beginning at day 2 after infection (Fig. 5B), demonstrating that vascular endothelial cells in the hemorrhage tissues produced both high-output RNS and ROS, and the temporal kinetics of their production coincided with hemorrhage development. These results strongly suggest that endothelial cell death occurring in the hemorrhage tissues is related to RNS and ROS production.

Endothelial cells support DENV replication and undergo apoptosis after infection. In vitro studies were performed to reveal the relationship between DENV infection of endothelial cells and endothelial cell death. Both MBECs and HUVECs were infected with DENV. As demonstrated by the presence of intracellular viral protein, 48.2% and 44.3% of HUVECs and MBECs, respectively, were infected by DENV (Fig. 6A). However, while DENV replication in MBECs peaked at 24 h and declined thereafter, that in human endothelial cells continued to rise up to 36 h after infection (Fig. 6B). These results show that both mouse and human endothelial cells supported productive viral infection, although the infection kinetics were different in these two types of primary endothelial cells. In the meantime, the endothelial cells became apoptotic, and the percentage of apoptotic cells was MOI dependent (Fig. 6C and D). Moreover, the addition of either zVAD-FMK or fumonisin B1, a ceramide inhibitor, significantly reduced DENV-induced cell death, indicating that DENV-induced endothelial cell death is caspase dependent and involves the activation of de novo ceramide synthesis (Fig. 6E). These results together indicate that endothelial cells of both human and mouse origin support DENV growth, and DENV induces endothelial cell apoptosis.

Endothelial cells produce iNOS and free radicals in response to DENV infection. To investigate whether DENV-induced apoptosis involves RNS production, HUVEC cells were infected with DENV, and iNOS expression was monitored. Western blot analysis showed that while eNOS was constitutively expressed and not affected by DENV infection, iNOS was induced in infected cells at 8 h after infection, and the level of expression continued to increase up to 16 h (Fig. 7A). In addition, NOx was produced in the culture supernatants of infected cells starting at 6 h after infection and peaked at 24 h (Fig. 7B). These results indicate that DENV infection induces endothelial cell iNOS expression and the production of high levels of RNS.

To determine whether DENV-induced apoptosis also involves ROS, DENV-infected HUVECs were labeled with DCFH-DA. As DCFH-DA is oxidized by ROS and/or RNS to produce dichlorofluorescein (DCF) cells expressing DCF are

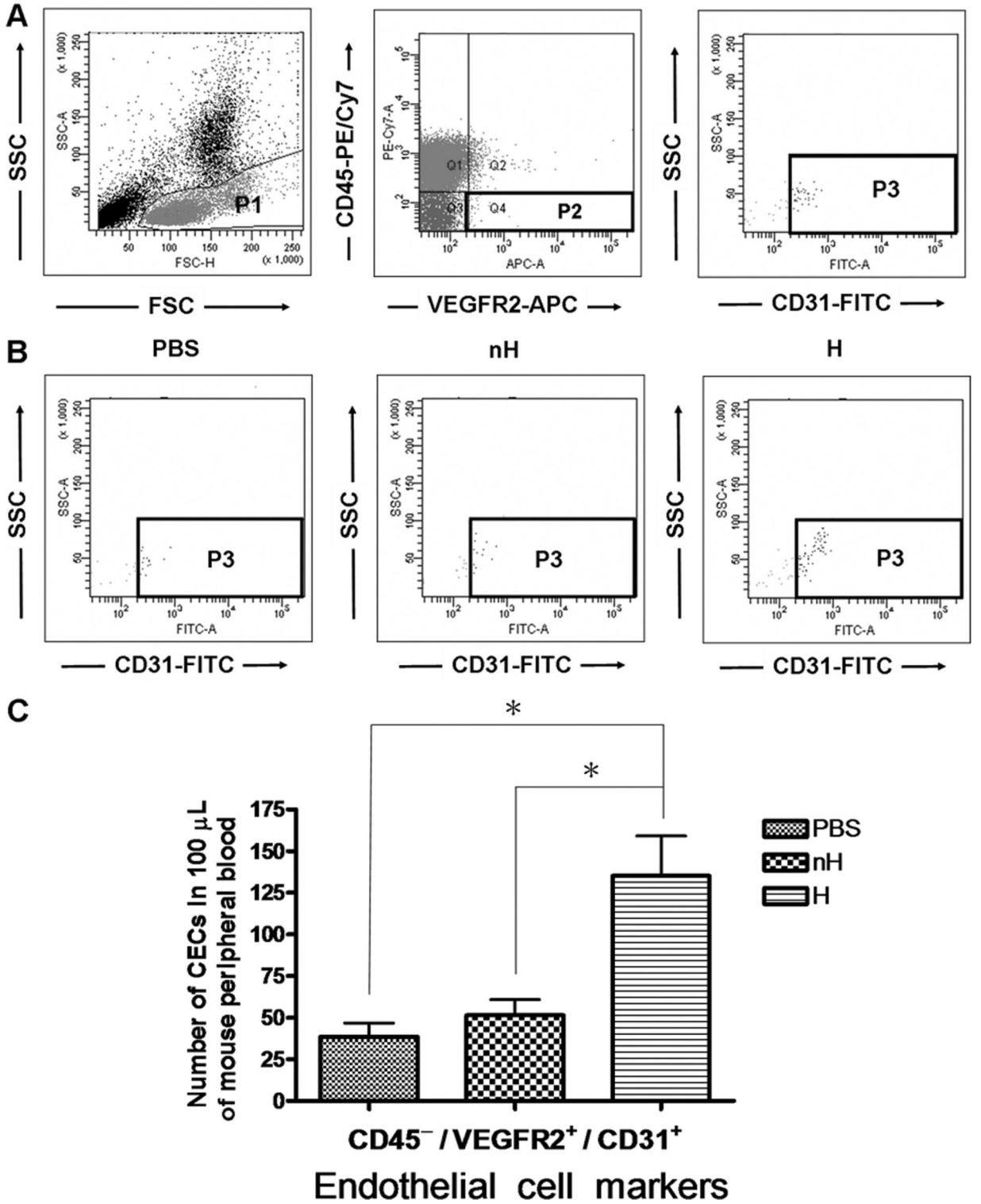

FIG. 4. Enumeration of CECs. Mice were inoculated intradermally with PBS or 2×10^9 PFU of DENV. Three days after infection, peripheral blood was collected, and the percentage of CEC was analyzed by flow cytometry. (A) Strategy for flow cytometric detection of CECs. In the P1 gate, cells were gated to exclude polymorphonuclear cells, dead cells, and debris. In the P2 gate, $CD45^-$ $VEGFR2^+$ cells were gated to exclude $CD45^+$ leukocytes. In the P3 gate, $VEGFR2^+$ $CD31^+$ cells were identified as being CECs. SSC, side scatter; FSC, forward scatter. (B) Dot plots showing representatives of the gated CECs in uninfected mice (PBS) and DENV-inoculated mice that did develop hemorrhage (H) or did not develop hemorrhage (nH), respectively. (C) Bar graphs showing the numbers of $CD45^-$ $VEGFR2^+$ $CD31^+$ cells in 100 μl of mouse peripheral blood. The data from three experiments were pooled. A total of 100,000 events were acquired for each specimen. *, $P < 0.05$.

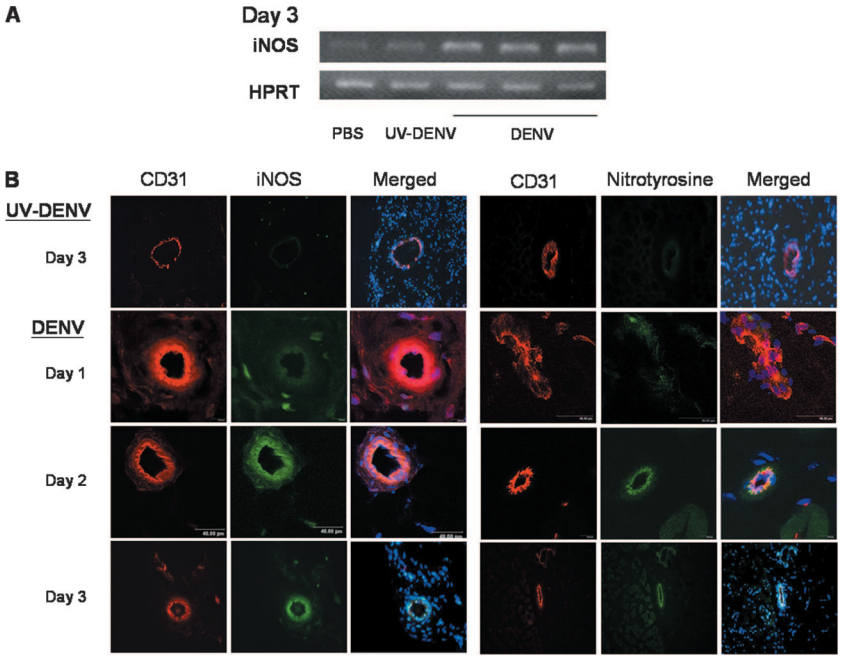

FIG. 5. Endothelial cells in hemorrhage tissues express iNOS and nitrotyrosine. (A) RNA was extracted from subcutaneous tissues of mice receiving PBS, 2×10^9 PFU of DENV, or an otherwise equivalent titer of UV-inactivated DENV at day 3 after inoculation. iNOS and HPRT mRNAs were amplified by RT-PCR. (B) Immunofluorescence staining was done on the cryosections of the subcutaneous tissues. The sections were stained with PE-conjugated rat anti-mouse CD31 antibody, FITC-conjugated rat anti-mouse iNOS antibody, and Hoechst 33258 stain or PE-conjugated rat anti-mouse CD31 antibody, rabbit anti-nitrotyrosine antibody, FITC-conjugated goat anti-rabbit antibody, and Hoechst 33258 stain. Immunofluorescence was viewed with a confocal microscope. Original magnification, ×630. The data presented are representative of five repeated experiments.

those that can produce ROS and/or RNS. Results show that free radical-producing endothelial cells increased in an MOI- and time-dependent manner (Fig. 7C and D). The results together indicate that DENV infection of endothelial cells induces the production of free radicals.

Blocking both RNS and ROS completely reverses DENV-induced cell death. iNOS-deficient endothelial cells and ROS inhibitors were employed to delineate the involvement of RNS and ROS in DENV-induced endothelial cell apoptosis. Results in Fig. 7E show that DENV-induced iNOS-deficient endothelial cell death was 17.6% ± 5% at 24 h after infection, half of that in the wild-type cells (33.7% ± 3%; $P < 0.05$), demonstrating that RNS are involved, although only partially, in DENV-induced endothelial cell death. Interestingly, while the treatment of endothelial cells with either NAC or L-NAME alone partially reduced DENV-induced endothelial cell death, the addition of both inhibitors completely reversed the effect of DENV on the cells (Fig. 7F). Therefore, the effect of DENV on endothelial cell death is through the combined activities of RNS and ROS.

TNF-α enhances DENV-induced apoptosis through increased production of both RNS and ROS. We have previously shown using TNF-$\alpha^{-/-}$ mice that TNF-α is critical to hemorrhage development in DENV-infected mice (9), and TNF-α increased DENV-induced endothelial cell death (Fig. 8A); experiments were performed to investigate the effect of TNF-α on endothelial cell production of iNOS and free radicals after DENV infection. The results show that while DENV at an MOI of 0.1 or TNF-α at 30 or 300 pg/ml alone induced the expression of low levels of iNOS and free radicals, the presence of both of them greatly increased their expression levels (Fig. 8B and C), indicating that the virus and TNF-α work synergistically in inducing iNOS and free radical production. Interestingly, the effect of TNF-α on DENV-induced endothelial cell death was reversed in the presence of NAC alone and with the combination of NAC and L-NAME (Fig. 8D). Moreover, zVAD-FMK reversed the effect of TNF-α on DENV-induced cell death (Fig. 8D). These results together indicate that the effect of TNF-α on DENV-induced endothelial cell apoptosis is through enhancing the production of both RNS and ROS, especially ROS.

A transwell assay was performed to further determine the relationships between endothelial cell apoptosis and permeability. Figure 9 shows that TNF-α alone and TNF-α plus DENV increased the permeability of the endothelial monolayer and that the addition of zVAD-FMK reduced the effects of TNF-α and TNF-α plus DENV on endothelial cell permeability to the level of controls. These results show that TNF-α-induced endothelial cell apoptosis and TNF-α-plus-DENV-induced endothelial cell apoptosis contribute to the loss of endothelial integrity.

RNS and ROS are critical to the development of dengue hemorrhage in mice. As we have shown that endothelial cells in hemorrhage tissues expressed iNOS and nitrotyrosine (Fig. 5A and B) and that blocking RNS and ROS production reversed TNF-α- and DENV-induced endothelial cell death in vitro (Fig. 8D), the roles of ROS and RNS in dengue hemorrhage were further investigated in the mouse model.

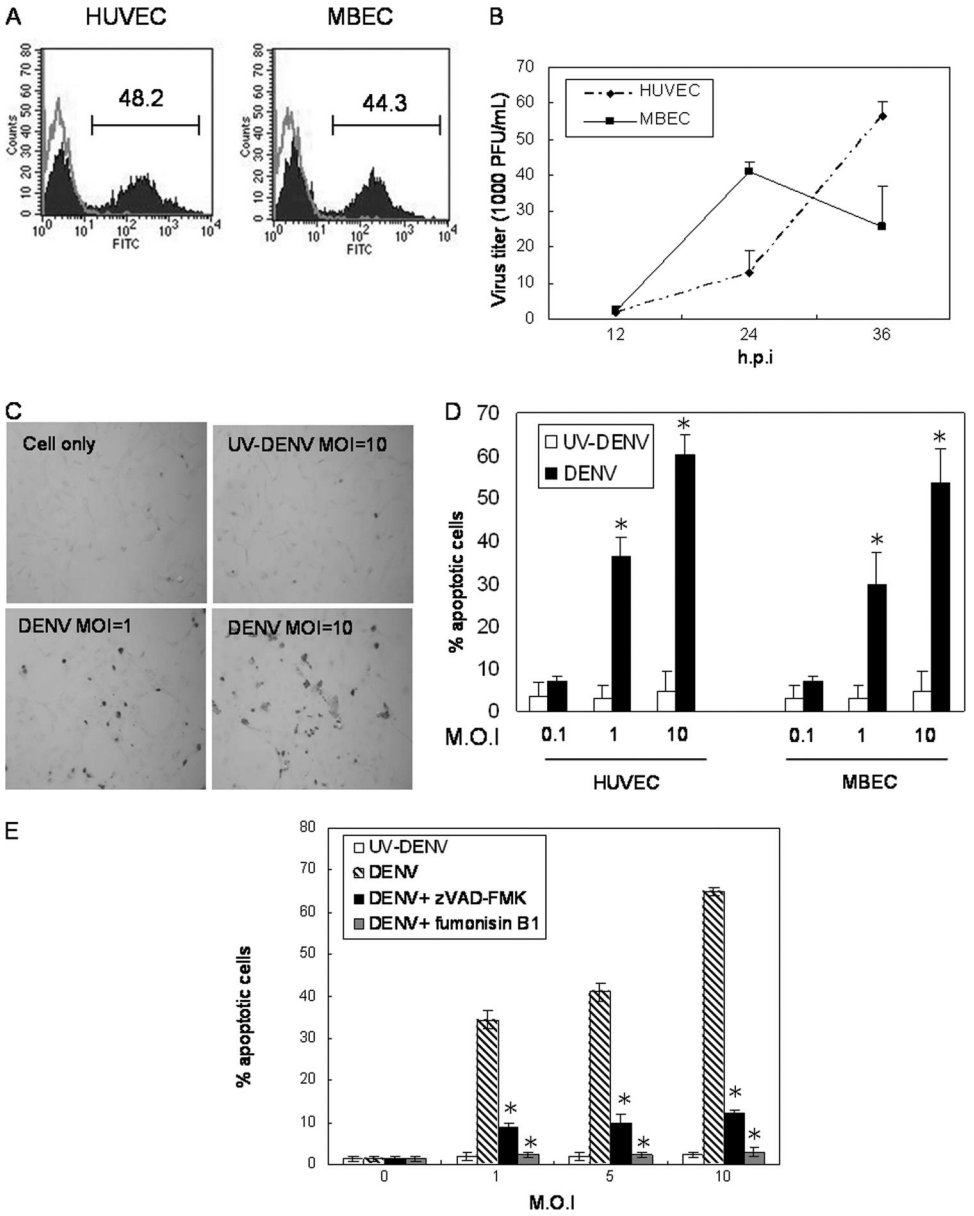

FIG. 6. DENV productively infects endothelial cells and induces apoptosis. (A) Both HUVECs and MBECs were infected with DENV at an MOI of 5. At 24 h after infection, cells were fixed, permeabilized, and stained with rabbit anti-DENV antibody plus FITC-conjugated goat anti-rabbit IgG. The gray line represents uninfected cells, and the darkened area indicates infected cells. The numbers indicate the percentages of cells that stained positive for DENV antigen. (B) Culture supernatants from DENV-infected HUVECs (diamond) and MBECs (square) (MOI of 5) were harvested at different time points after infection. The virus titer was determined by plaque assay. Data from three independent experiments were pooled and are shown as means plus standard deviations (SD). h.p.i, hours postinfection. (C) HUVECs were infected with DENV at an MOI of 1 or 10 or cultured with UV-inactivated DENV at an otherwise equivalent MOI of 10. At 24 h after incubation, cells were stained with TUNEL reaction mixtures as described in Materials and Methods. Cells stained brown are counted as being TUNEL$^+$. Original magnification, ×200. (D) Comparison of the percent apoptotic cells in HUVECs and MBECs infected by DENV at different MOIs. Percentages of apoptotic cells were obtained by dividing TUNEL$^+$ cells by the total number of cells counted. At least 1,000 cells in the each monolayer were counted. Data shown are the mean values plus SD of numbers pooled from three independent experiments. *, $P < 0.05$ (comparing the percent apoptotic cells in the DENV-infected monolayer to that in the UV-inactivated DENV monolayer). (E) Cells were infected with DENV at an MOI of 1, 5, or 10 and cultured in the absence (hatched bar) or presence of 4 μM zVAD-FMK (darkened bar) or 25 μM fumonisin B1 (gray bar) for 30 min before infection and throughout the course of the experiment. Cultures with UV-inactivated DENV were used as controls (open bar). Percentages of apoptotic cells were obtained by dividing the numbers of TUNEL$^+$ cells by the total number of cells counted. At least 1,000 cells in each monolayer were counted. Data shown are the mean values plus SD of the percent apoptotic cells pooled from three independent experiments. *, $P < 0.05$ (comparing percent apoptotic cells in the zVAD-FMK- or fumonisin B1-treated DENV-infected monolayer to that in the control DENV-infected monolayer).

P47$^{phox-/-}$, iNOS $^{-/-}$, and wild-type mice were infected intradermally with 2×10^9 PFU of DENV. Separate groups of the infected iNOS$^{-/-}$ and wild-type mice were fed with drinking water containing apocynin. While 77.8% of the wild-type mice infected with DENV developed systemic and severe hemorrhage, 28.6% of wild-type mice treated with apocynin, 33.3% of iNOS$^{-/-}$ mice without apocynin treatment, and 21.4% of apocynin-treated iNOS$^{-/-}$ mice devel-

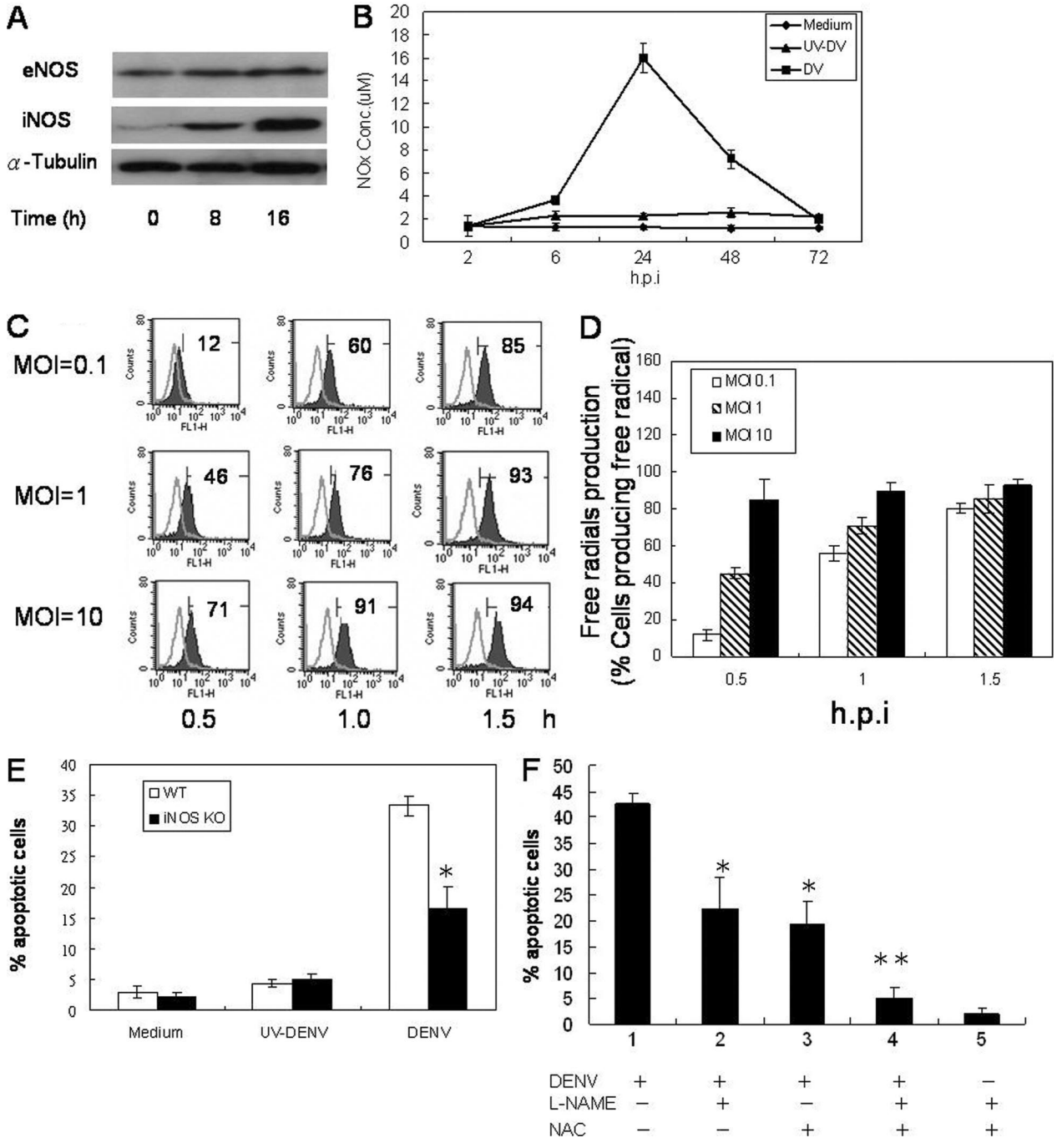

FIG. 7. DENV infection of endothelial cells induces iNOS expression and RNS and ROS production. (A) HUVECs were infected by DENV at an MOI of 1, and cells were harvested at 0, 8, and 16 h after infection. eNOS, iNOS, and α-tubulin expression levels were determined by Western blot analysis. The ratios of eNOS/tubulin were 0.8, 0.8, and 0.8 and those of iNOS/tubulin were 0.1, 0.8, and 1.1 at 0, 8, and 16 h after infection, respectively. (B) Supernatants from DENV-infected HUVECs at an MOI of 1 were collected at different time points after infection, and the NOx concentration was determined by a Griess assay. (C) HUVEC cultures were infected with DENV at an MOI of 0.1, 1, or 10 and incubated in the presence of DCFH (5 μM), which is converted to the fluorescent product DCF by ROS, for 30 min. Histograms show DCF fluorescence intensity at 0.5, 1.0, and 1.5 h after DENV infection. The numbers indicate the percentages of cells producing free radicals. (D) Bar graphs showing mean percentages of HUVECs producing free radicals at 0.5, 1.0, and 1.5 h after infection by DENV at different MOIs. The data shown are the mean values plus SD pooled from four independent experiments. The data show that the percentage of free radical-producing cells increased in a time- and MOI-dependent manner. h.p.i, hours postinfection. (E) Wild-type (WT) or iNOS$^{-/-}$ murine endothelial cells were infected with DENV or an otherwise equivalent titer of UV-inactivated DENV at an MOI of 1. At 24 h after infection, the percentage of TUNEL^{+} apoptotic cells was determined by counting 1,000 cells per slide. Data shown are the mean values ± SD pooled from three independent experiments. *, $P < 0.05$ (comparing MBEC harvested from iNOS$^{-/-}$ mice to that from wild-type mice). KO, knockout. (F) Cells were pretreated with L-NAME (10 μM), NAC (15 μM), or both for 30 min and then infected with DENV at an MOI of 5. Cells treated with L-NAME and NAC without infection were used as controls. At 24 h after incubation, the percentage of TUNEL reaction-positive apoptotic cells was determined by counting 1,000 cells per slide. Data shown are the mean values ± SD pooled from three independent experiments. *, $P < 0.05$; **, $P < 0.005$ (comparing L-NAME- and NAC-treated DENV-infected cells to DENV-infected cells without treatment).

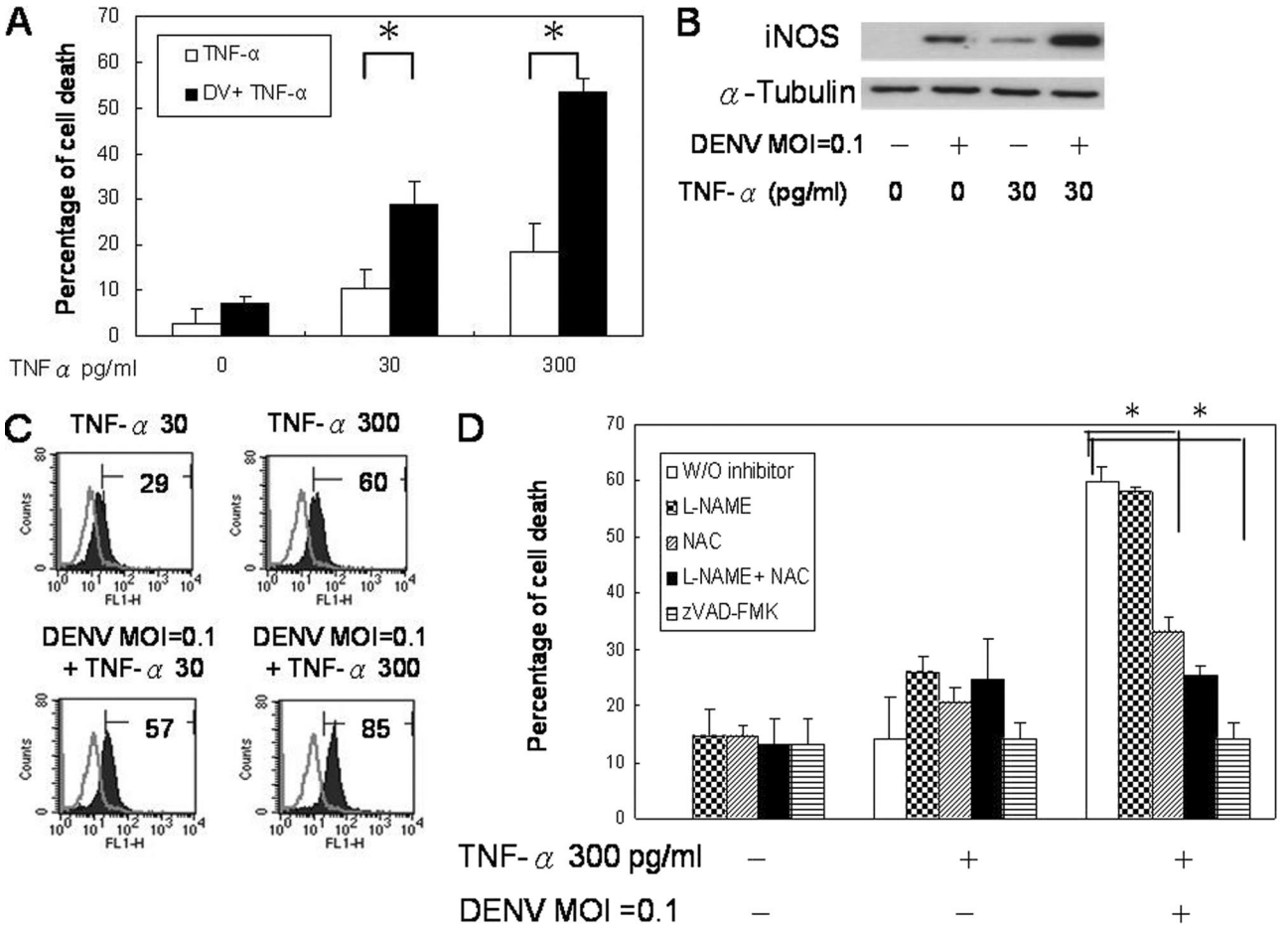

FIG. 8. TNF-α enhances DENV-induced endothelial cell apoptosis through augmentation of ROS and RNS production. (A) HUVEC cultures with or without TNF-α treatment were infected with DENV (DV) at an MOI of 0.1. Cell viability was determined by MTT assay at 24 h after infection. (B) HUVECs were treated with or without TNF-α for 6 h before infection with DENV at an MOI of 0.1. Cells were harvested at 24 h after infection, and cell lysates were subjected to Western blot analysis for iNOS and α-tubulin expression levels. The results shown are representative of five repeated experiments. (C) HUVEC cultures were treated with different concentrations of TNF-α for 6 h before infection with DENV at an MOI of 1. Cells were incubated in the presence of DCFH (5 μM) for 30 min. Histograms show DCF fluorescence intensity. Gray line, uninfected control; darkened area, DENV-infected HUVECs. The numbers indicate the percentages of cells producing free radicals. The histogram shown is representative of data from four repeated experiments. (D) HUVEC cultures were pretreated with L-NAME (10 nM), NAC (15 nM), both L-NAME and NAC, or zVAD-FMK (4 μM) or without any inhibitor for 2 h prior to the addition of TNF-α (300 pg/ml) and DENV (MOI of 0.1). Cell viability was determined by MTT assay. Data shown are the means plus SD of data pooled from three independent experiments. *, $P < 0.05$.

oped mild and local hemorrhage (Fig. 10). Interestingly, none of the p47$^{phox-/-}$ mice had hemorrhage manifestations. These results strongly indicate that RNS as well as ROS are involved in DENV-induced hemorrhage in the mouse model and that blocking the production of RNS and ROS greatly reduces hemorrhage development, pointing to the possibility that antioxidant treatment may be effective in preventing hemorrhage development in DENV-infected individuals.

DISCUSSION

DHF represents a severe clinical manifestation of DENV infection. The features that distinguish DHF from dengue fever include an increase of vascular permeability, thrombocytopenia, and bleeding manifestations (4, 20). The pathogenic mechanisms underlying vascular damage and hemorrhage remain ill defined. In the present study, employing our dengue hemorrhage mouse model and in vitro endothelial cell culture systems, we established in temporal sequence that (i) DENV infecting the endothelium, (ii) TNF-α stimulating endothelial cells, (iii) endothelial cells expressing iNOS and nitrotyrosine, and (iv) endothelial cells undergoing apoptosis are important events that lead to hemorrhage development.

Vascular endothelial cell involvement is important in viral hemorrhage (48). Hemorrhagic virus targeting endothelial cells may directly or indirectly lead to hemorrhage (47, 48). In Ebola virus-infected cynomolgus monkeys, endothelial cells are not the targets of the virus during the early phases of infection; persistent viral replication in the endothelial cells is evident only after the onset of disseminated intravascular coagulation, showing that hemorrhage is not a direct effect of the

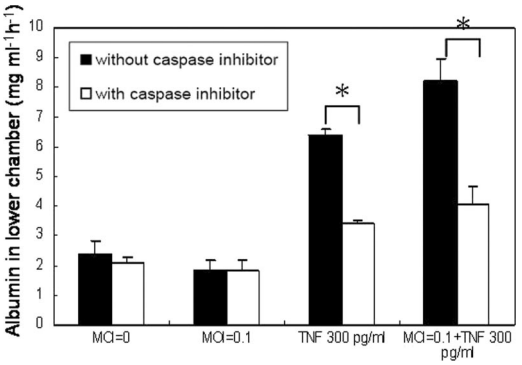

FIG. 9. Endothelial cell apoptosis contributes to permeability change. HUVEC monolayers in the transwell chamber with and without zVAD-FMK (4 μM) treatment were infected with DENV (MOI of 0.1), were treated with TNF-α (300 pg/ml), received both DENV and TNF-α, or received neither and incubated for 24 h. One hundred microliters of trypan blue-stained bovine serum albumin was added to the upper chamber of the transwell 30 min before the upper chambers were removed. The absorbance of the solution in the lower chamber was measured at 595 nm. Results are expressed as the amount of bovine serum albumin detected in the lower chamber. *, $P < 0.05$ (comparing the group without caspase treatment to that with caspase treatment).

virus-induced cytolysis of endothelial cells (16). Hantaviruses, including both pathogenic and nonpathogenic strains, replicate primarily in endothelial cells but cause no apparent cytopathic effects (47, 54). Therefore, the hypothesis is that virus targeting endothelial cells and immune mechanisms are both important in the pathogenesis of the disease (46). Dendritic cells and monocytes/macrophages are believed to be the major targets of DENV in the human host (52). However, DENV antigens can be detected not only in the macrophages but also in the endothelial cells in patients who died of DHF (5, 21, 30). Concurrent with finding for humans, our mouse model revealed DENV antigen in endothelial cells and in in vitro primary cultures. By probing the presence of DENV NS1 and nucleic acids, we further demonstrated that DENV actively infects mouse endothelial cells (23, 40, 43). With that, mouse can be added to the list of primary endothelial cells that support DENV replication (2, 6, 36). Importantly, as a result of the DENV interaction with the endothelial cells and in the presence of TNF-α, endothelial cells undergo apoptosis (Fig. 8A) (3).

A recent report by Limonta et al. demonstrated apoptotic cells in tissues from five of six fatal DSS cases (37). Apoptotic cerebral cells, leukocytes, and intestinal and pulmonary microvascular endothelial cells were found in these fatal cases, which suggests that apoptosis may be related to vascular leakage. Thus, the contribution of endothelial cell apoptosis to the pathogenic mechanism of DHF/DSS is considered. In the present study, we demonstrated that the endothelial cells in hemorrhagic mouse tissue are apoptotic soon before and at the time of hemorrhage development (Fig. 2C); caspase inhibitor reduces the permeability change induced by DENV infection and TNF-α treatment in vitro (Fig. 9) as well as the percentage and severity of hemorrhage in vivo (Fig. 3). Furthermore, the temporal kinetics of endothelial cells expressing iNOS and nitrotyrosine correspond to hemorrhage development (Fig. 5B) and deficiency in iNOS or $p47^{phox}$ or an oxidase inhibitor separately reduces the incidence and severity of hemorrhage (Fig. 10). These data together strongly indicate that endothelial cell apoptosis, which contributes to the loss of vascular integrity, is critical to hemorrhage development and that it is mediated by RNS and ROS.

It was shown previously that hepatitis C virus, another member of the *Flaviviridae*, causes double-strand DNA damage and cellular gene mutation through the production of RNS and ROS (41, 42). UV-inactivated Japanese encephalitis virus induces mouse neuroblastoma N18 and human neuronal NT-2 cell death through ROS and NF-κB activation (38). In the present study, we showed that endothelial cells infected by

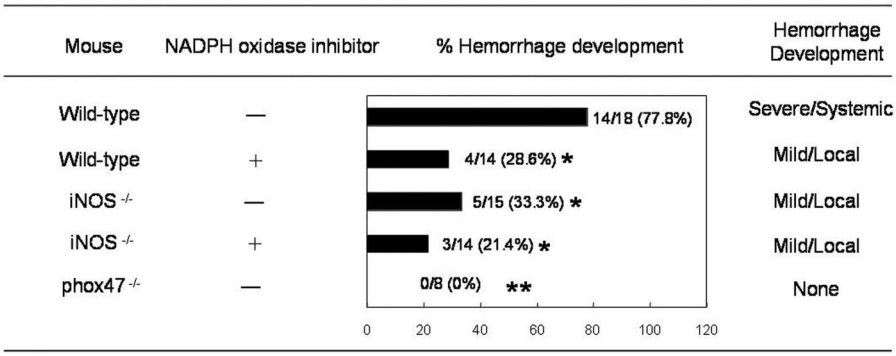

FIG. 10. Both RNS and ROS contribute to hemorrhage development in DENV-infected mice. Wild-type, $iNOS^{-/-}$, or $p47^{phox-/-}$ mice were inoculated with 2×10^9 PFU of DENV intradermally. Separate groups of wild-type and $iNOS^{-/-}$ mice were fed with drinking water containing apocynin (40 mg/ml), an NADPH oxidase inhibitor, starting 5 days previously and continued after intradermal DENV inoculation until termination of the experiment. Hemorrhage development was observed when mice were killed at 3 days after DENV inoculation. Percent hemorrhage development was obtained by dividing the number of mice that developed hemorrhage with the total number of mice inoculated with DENV. Hemorrhage that developed in the skin or subcutaneous tissues on the upper back of the mouse is referred to as mild/local hemorrhage, and that which developed at multiple anatomical sites is referred to as severe/systemic hemorrhage. The *P* value obtained by comparing $p47^{phox-/-}$ to wild-type mice is <0.0001 (**), and that obtained by comparing wild-type, $iNOS^{-/-}$, or $iNOS^{-/-}$ mice treated with apocynin to wild-type mice is <0.05 (*). The comparison between apocynin-treated wild-type mice or $iNOS^{-/-}$ mice treated with apocynin and $iNOS^{-/-}$ mice did not achieve statistical significance. The data from two to three experiments were pooled.

DENV express iNOS and produce RNS and ROS (Fig. 7A to D). The addition of TNF-α enhances DENV-infected endothelial cell iNOS expression and high levels RNS and ROS production and in the meantime enhances virus-induced apoptosis (Fig. 8A and B). The addition of NAC and L-NAME reverses the effects of TNF-α and DENV on endothelial cells (Fig. 8D). The present study is the first to demonstrate that TNF-α enhances the effect of DENV on endothelial cells through an augmentation of RNS and ROS production, and such an effect is critical for vascular damage in vivo.

Oxidative stress is known to be a shared risk factor of many vascular disorders such as atherosclerosis, reperfusion injury, and heart failure (11), and oxidase-mediated reactions are the major source of ROS in endothelial cells (17, 18, 35). Li and Shah previously investigated the molecular nature of oxidase in human, bovine, and porcine endothelial cells and found that endothelial cells oxidase is preferentially NADPH dependent rather than NADH dependent (35). It was previously reported that the NADPH oxidase subunit $p47^{phox}$ plays an essential role in endothelial cell ROS production in response to TNF-α (34) and that ROS mediates TNF-α-induced human endothelial cell apoptosis (12). $p47^{phox}$ phosphorylation and the subsequent translocation to the membrane are critical for the activation of endothelial cells NADPH oxidase induced by TNF-α (13, 33). It was previously suggested that TNF-α activates protein kinase C ζ, which in turn phosphorylates $p47^{phox}$, thereby inducing the translocation of this subunit to the membrane, where it is associated with $gp91^{phox}$ to form the active enzyme complex (28). Since ceramide is able to activate protein kinase C ζ, it is possible that ceramide employs this kinase to regulate NADPH oxidase in the endothelial cells or that ceramide-enriched membrane platforms recruit the subunits of NADPH oxidase to assemble at the cell membrane after TNF-α treatment (8). It was shown previously that infection of neuronal and hepatoma cell lines by DENV induces apoptosis through NADPH oxidase activation and ROS production (29, 45). Our in vitro study showed that DENV induces endothelial cell free radical production and apoptosis (Fig. 7C and D) and that endothelial cell apoptosis is suppressed by a ceramide synthesis inhibitor, fumonisin B1 (Fig. 6E). In addition, TNF-α enhances DENV-induced free radical production in endothelial cells and their susceptibility to apoptosis (Fig. 8A to D). It was previously reported that TNF-α synergizes with gamma interferon in inducing β-cell apoptosis through the enhanced production of intracellular ROS (31). It is our speculation that TNF-α synergistically enhances DENV-induced ROS production through the ceramide-NADPH pathway in endothelial cells.

Peroxynitrite, produced by the reaction of nitric oxide and superoxide radicals, is a short-lived oxidant species that potently induces cell death (50). It causes damage through oxidation, nitration, and nitrosation (50). Tyrosine nitration, as indicated by the presence of nitrotyrosine in tissues, has been shown to play pathological roles in circulatory shock, type 1 diabetes, diabetic complications, and chronic heart failure (50). Although it has been shown that DENV patients experience oxidative stress and that blood NO levels are high (51), this study is the first to show in vivo that endothelial cells in hemorrhage tissues are damaged by tyrosine nitration. Importantly, the inhibition of RNS and ROS production, and, thus, the formation of peroxynitrite, is beneficial to hosts infected with DENV.

In summary, by using a dengue hemorrhage mouse model and in vitro endothelial cell cultures, we demonstrated that DENV and TNF-α together induce endothelial cell apoptosis through the production of RNS and ROS. The reaction of RNS and ROS, damaging endothelial cells through tyrosine nitration, leads to hemorrhage development. The inhibition of RNS and ROS greatly reduces hemorrhage. The present study reveals the molecular basis for the pathogenesis of dengue hemorrhage and sheds light on potential treatment strategies for dengue hemorrhage.

ACKNOWLEDGMENTS

We thank Chwan-Chuen King and Shu-Ching Chen for helpful discussions and suggestions.

This work was supported by NRPGM grant NSC-96-3112-B-002-016 and NHRI grant NHRI-CN-CL9302P of the Republic of China to B.A.W.-H. We acknowledge the support provided by the Seventh Core Lab of the Department of Medical Research of National Taiwan University Hospital.

REFERENCES

1. **Allen, H. L., and G. S. Deepe, Jr.** 2005. Apoptosis modulates protective immunity to the pathogenic fungus Histoplasma capsulatum. J. Clin. Investig. **115:**2875–2885.
2. **Andrews, B. S., A. N. Theofilopoulos, C. J. Peters, D. J. Loskutoff, W. E. Brandt, and F. J. Dixon.** 1978. Replication of dengue and Junin viruses in cultured rabbit and human endothelial cells. Infect. Immun. **20:**776–781.
3. **Avirutnan, P., P. Malasit, B. Seliger, S. Bhakdi, and M. Husmann.** 1998. Dengue virus infection of human endothelial cells leads to chemokine production, complement activation, and apoptosis. J. Immunol. **161:**6338–6346.

3a. **Bethell, D. B., K. Flobbe, X. T. Cao, N. P. Day, T. P. Pham, W. A. Buurman, M. J. Cardosa, N. J. White, and D. Kwiatkowski.** 1998. Pathophysiologic and prognostic role of cytokines in dengue hemorrhagic fever. J. Infect. Dis. **177:**778–782.

4. **Bhamarapravati, N.** 1989. Hemostatic defects in dengue hemorrhagic fever. Rev. Infect. Dis. **11**(Suppl. 4)**:**S826–S829.
5. **Bhoopat, L., N. Bhamarapravati, C. Attasiri, S. Yoksarn, B. Chaiwun, S. Khunamornpong, and V. Sirisanthana.** 1996. Immunohistochemical characterization of a new monoclonal antibody reactive with dengue virus-infected cells in frozen tissue using immunoperoxidase technique. Asian Pac. J. Allergy Immunol. **14:**107–113.
6. **Bonner, S. M., and M. A. O'Sullivan.** 1998. Endothelial cell monolayers as a model system to investigate dengue shock syndrome. J. Virol. Methods **71:**159–167.
7. **Cardier, J. E., B. Rivas, E. Romano, A. L. Rothman, C. Perez-Perez, M. Ochoa, A. M. Caceres, M. Cardier, N. Guevara, and R. Giovannetti.** 2006. Evidence of vascular damage in dengue disease: demonstration of high levels of soluble cell adhesion molecules and circulating endothelial cells. Endothelium **13:**335–340.
8. **Chatterjee, S.** 1998. Sphingolipids in atherosclerosis and vascular biology. Arterioscler. Thromb. Vasc. Biol. **18:**1523–1533.
9. **Chen, H.-C., F. M. Hofman, J. T. Kung, Y.-D. Lin, and B. A. Wu-Hsieh.** 2007. Both virus and tumor necrosis factor alpha are critical for endothelium damage in a mouse model of dengue virus-induced hemorrhage. J. Virol. **81:**5518–5526.
10. **Cines, D. B., E. S. Pollak, C. A. Buck, J. Loscalzo, G. A. Zimmerman, R. P. McEver, J. S. Pober, T. M. Wick, B. A. Konkle, B. S. Schwartz, E. S. Barnathan, K. R. McCrae, B. A. Hug, A. M. Schmidt, and D. M. Stern.** 1998. Endothelial cells in physiology and in the pathophysiology of vascular disorders. Blood **91:**3527–3561.
11. **Davidson, S. M., and M. R. Duchen.** 2007. Endothelial mitochondria: contributing to vascular function and disease. Circ. Res. **100:**1128–1141.
12. **Deshpande, S. S., P. Angkeow, J. Huang, M. Ozaki, and K. Irani.** 2000. Rac1 inhibits TNF-alpha-induced endothelial cell apoptosis: dual regulation by reactive oxygen species. FASEB J. **14:**1705–1714.
13. **Dewas, C., P. M. Dang, M. A. Gougerot-Pocidalo, and J. El-Benna.** 2003. TNF-alpha induces phosphorylation of p47(phox) in human neutrophils: partial phosphorylation of p47phox is a common event of priming of human neutrophils by TNF-alpha and granulocyte-macrophage colony-stimulating factor. J. Immunol. **171:**4392–4398.
14. **Erdbruegger, U., M. Haubitz, and A. Woywodt.** 2006. Circulating endothelial cells: a novel marker of endothelial damage. Clin. Chim. Acta **373:**17–26.
15. **Fernandez-Mestre, M. T., K. Gendzekhadze, P. Rivas-Vetencourt, and Z.**

Layrisse. 2004. TNF-alpha-308A allele, a possible severity risk factor of hemorrhagic manifestation in dengue fever patients. Tissue Antigens **64:** 469–472.
16. **Geisbert, T. W., H. A. Young, P. B. Jahrling, K. J. Davis, T. Larsen, E. Kagan, and L. E. Hensley.** 2003. Pathogenesis of Ebola hemorrhagic fever in primate models: evidence that hemorrhage is not a direct effect of virus-induced cytolysis of endothelial cells. Am. J. Pathol. **163:**2371–2382.
17. **Gorlach, A., R. P. Brandes, K. Nguyen, M. Amidi, F. Dehghani, and R. Busse.** 2000. A gp91phox containing NADPH oxidase selectively expressed in endothelial cells is a major source of oxygen radical generation in the arterial wall. Circ. Res. **87:**26–32.
18. **Griendling, K. K., D. Sorescu, and M. Ushio-Fukai.** 2000. NAD(P)H oxidase: role in cardiovascular biology and disease. Circ. Res. **86:**494–501.
19. **Grundmann, M., A. Woywodt, T. Kirsch, B. Hollwitz, K. Oehler, U. Erdbruegger, H. Haller, and M. Haubitz.** 2008. Circulating endothelial cells: a marker of vascular damage in patients with preeclampsia. Am. J. Obstet. Gynecol. **198:**317.e1–317.e5.
20. **Gubler, D. J.** 1998. Dengue and dengue hemorrhagic fever. Clin. Microbiol. Rev. **11:**480–496.
21. **Hall, W. C., T. P. Crowell, D. M. Watts, V. L. Barros, H. Kruger, F. Pinheiro, and C. J. Peters.** 1991. Demonstration of yellow fever and dengue antigens in formalin-fixed paraffin-embedded human liver by immunohistochemical analysis. Am. J. Trop. Med. Hyg. **45:**408–417.
22. **Haubitz, M., and A. Woywodt.** 2004. Circulating endothelial cells and vasculitis. Intern. Med. **43:**660–667.
23. **Henchal, E. A., S. L. Polo, V. Vorndam, C. Yaemsiri, B. L. Innis, and C. H. Hoke.** 1991. Sensitivity and specificity of a universal primer set for the rapid diagnosis of dengue virus infections by polymerase chain reaction and nucleic acid hybridization. Am. J. Trop. Med. Hyg. **45:**418–428.
24. **Holmes, E. C., and S. S. Twiddy.** 2003. The origin, emergence and evolutionary genetics of dengue virus. Infect. Genet. Evol. **3:**19–28.
25. **Hougee, S., A. Hartog, A. Sanders, Y. M. Graus, M. A. Hoijer, J. Garssen, W. B. van den Berg, H. M. van Beuningen, and H. F. Smit.** 2006. Oral administration of the NADPH-oxidase inhibitor apocynin partially restores diminished cartilage proteoglycan synthesis and reduces inflammation in mice. Eur. J. Pharmacol. **531:**264–269.
26. **Jackson, S. H., J. I. Gallin, and S. M. Holland.** 1995. The p47phox mouse knock-out model of chronic granulomatous disease. J. Exp. Med. **182:**751–758.
27. **Jaffe, E. A., R. L. Nachman, C. G. Becker, and C. R. Minick.** 1973. Culture of human endothelial cells derived from umbilical veins. Identification by morphologic and immunologic criteria. J. Clin. Investig. **52:**2745–2756.
28. **Jaffrey, S. R., and S. H. Snyder.** 1995. Nitric oxide: a neural messenger. Annu. Rev. Cell Dev. Biol. **11:**417–440.
29. **Jan, J.-T., B.-H. Chen, S.-H. Ma, C.-I. Liu, H.-P. Tsai, H.-C. Wu, S.-Y. Jiang, K.-D. Yang, and M.-F. Shaio.** 2000. Potential dengue virus-triggered apoptotic pathway in human neuroblastoma cells: arachidonic acid, superoxide anion, and NF-κB are sequentially involved. J. Virol. **74:**8680–8691.
30. **Jessie, K., M. Y. Fong, S. Devi, S. K. Lam, and K. T. Wong.** 2004. Localization of dengue virus in naturally infected human tissues, by immunohistochemistry and in situ hybridization. J. Infect. Dis. **189:**1411–1418.
31. **Kim, W. H., J. W. Lee, B. Gao, and M. H. Jung.** 2005. Synergistic activation of JNK/SAPK induced by TNF-alpha and IFN-gamma: apoptosis of pancreatic beta-cells via the p53 and ROS pathway. Cell. Signal. **17:**1516–1532.
32. **Kurane, I.** 2003. Dengue virus. Nippon Rinsho **61**(Suppl. 3)**:**486–490. (In Japanese.)
33. **Li, J.-M., L. M. Fan, M. R. Christie, and A. M. Shah.** 2005. Acute tumor necrosis factor alpha signaling via NADPH oxidase in microvascular endothelial cells: role of $p47^{phox}$ phosphorylation and binding to TRAF4. Mol. Cell. Biol. **25:**2320–2330.
34. **Li, J. M., A. M. Mullen, S. Yun, F. Wientjes, G. Y. Brouns, A. J. Thrasher, and A. M. Shah.** 2002. Essential role of the NADPH oxidase subunit p47(phox) in endothelial cell superoxide production in response to phorbol ester and tumor necrosis factor-alpha. Circ. Res. **90:**143–150.
35. **Li, J. M., and A. M. Shah.** 2001. Differential NADPH- versus NADH-dependent superoxide production by phagocyte-type endothelial cell NADPH oxidase. Cardiovasc. Res. **52:**477–486.
36. **Liew, K. J., and V. T. Chow.** 2004. Differential display RT-PCR analysis of ECV304 endothelial-like cells infected with dengue virus type 2 reveals messenger RNA expression profiles of multiple human genes involved in known and novel roles. J. Med. Virol. **72:**597–609.
37. **Limonta, D., V. Capo, G. Torres, A. B. Perez, and M. G. Guzman.** 2007. Apoptosis in tissues from fatal dengue shock syndrome. J. Clin. Virol. **40:** 50–54.
38. **Lin, R. J., C. L. Liao, and Y. L. Lin.** 2004. Replication-incompetent virions of Japanese encephalitis virus trigger neuronal cell death by oxidative stress in a culture system. J. Gen. Virol. **85:**521–533.
39. **Lucchina, L. C., M. E. Wilson, and L. A. Drake.** 1997. Dermatology and the recently returned traveler: infectious diseases with dermatologic manifestations. Int. J. Dermatol. **36:**167–181.
40. **Lucia, H. L., and D. Kangwanpong.** 1994. Identification of dengue virus-infected cells in paraffin-embedded tissue using in situ polymerase chain reaction and DNA hybridization. J. Virol. Methods **48:**1–8.
41. **Machida, K., K. T. Cheng, V. M. Sung, K. J. Lee, A. M. Levine, and M. M. Lai.** 2004. Hepatitis C virus infection activates the immunologic (type II) isoform of nitric oxide synthase and thereby enhances DNA damage and mutations of cellular genes. J. Virol. **78:**8835–8843.
42. **Machida, K., K. T. Cheng, V. M. Sung, A. M. Levine, S. Foung, and M. M. Lai.** 2006. Hepatitis C virus induces Toll-like receptor 4 expression, leading to enhanced production of beta interferon and interleukin-6. J. Virol. **80:** 866–874.
43. **Mackenzie, J. M., M. K. Jones, and P. R. Young.** 1996. Immunolocalization of the dengue virus nonstructural glycoprotein NS1 suggests a role in viral RNA replication. Virology **220:**232–240.
44. **Maffei, C. M., L. F. Mirels, R. A. Sobel, K. V. Clemons, and D. A. Stevens.** 2004. Cytokine and inducible nitric oxide synthase mRNA expression during experimental murine cryptococcal meningoencephalitis. Infect. Immun. **72:** 2338–2349.
45. **Marianneau, P., A. Cardona, L. Edelman, V. Deubel, and P. Despres.** 1997. Dengue virus replication in human hepatoma cells activates NF-κB which in turn induces apoptotic cell death. J. Virol. **71:**3244–3249.
46. **Mori, M., A. L. Rothman, I. Kurane, J. M. Montoya, K. B. Nolte, J. E. Norman, D. C. Waite, F. T. Koster, and F. A. Ennis.** 1999. High levels of cytokine-producing cells in the lung tissues of patients with fatal hantavirus pulmonary syndrome. J. Infect. Dis. **179:**295–302.
47. **Pensiero, M. N., J. B. Sharefkin, C. W. Dieffenbach, and J. Hay.** 1992. Hantaan virus infection of human endothelial cells. J. Virol. **66:**5929–5936.
48. **Peters, C. J., and S. R. Zaki.** 2002. Role of the endothelium in viral hemorrhagic fevers. Crit. Care Med. **30:**S268–S273.
49. **Rigau-Perez, J. G., G. G. Clark, D. J. Gubler, P. Reiter, E. J. Sanders, and A. V. Vorndam.** 1998. Dengue and dengue haemorrhagic fever. Lancet **352:** 971–977.
50. **Szabo, C., H. Ischiropoulos, and R. Radi.** 2007. Peroxynitrite: biochemistry, pathophysiology and development of therapeutics. Nat. Rev. Drug Discov. **6:**662–680.
51. **Valero, N., L. M. Espina, G. Anez, E. Torres, and J. A. Mosquera.** 2002. Short report: increased level of serum nitric oxide in patients with dengue. Am. J. Trop. Med. Hyg. **66:**762–764.
52. **Wu, S. J., G. Grouard-Vogel, W. Sun, J. R. Mascola, E. Brachtel, R. Putvatana, M. K. Louder, L. Filgueira, M. A. Marovich, H. K. Wong, A. Blauvelt, G. S. Murphy, M. L. Robb, B. L. Innes, D. L. Birx, C. G. Hayes, and S. S. Frankel.** 2000. Human skin Langerhans cells are targets of dengue virus infection. Nat. Med. **6:**816–820.
53. **Wu, Z., F. M. Hofman, and B. V. Zlokovic.** 2003. A simple method for isolation and characterization of mouse brain microvascular endothelial cells. J. Neurosci. Methods **130:**53–63.
54. **Yanagihara, R., and D. J. Silverman.** 1990. Experimental infection of human vascular endothelial cells by pathogenic and nonpathogenic hantaviruses. Arch. Virol. **111:**281–286.
55. **Yen, Y.-T., F. Liao, C.-H. Hsiao, C.-L. Kao, Y.-C. Chen, and B. A. Wu-Hsieh.** 2006. Modeling the early events of severe acute respiratory syndrome coronavirus infection in vitro. J. Virol. **80:**2684–2693.